Aerodynamic Force Measurement in a Large-Scale Shock Tunnel

Yunpeng Wang, Yunfeng Liu, Changtong Luo, and Zonglin Jiang

Abstract Force tests were conducted at the long-duration-test shock tunnel JF12, which has been designed and built in the Institute of Mechanics, Chinese Academy of Sciences. The performance tests demonstrated that this facility is capable of reproducing a flow of dry air at Mach numbers from 5 to 9 at more than 100 ms test duration. Therefore, the traditional internal strain-gauge balance was considered for the force tests used in this large impulse facility. However, when the force tests are conducted in a shock tunnel, the inertial forces lead to low-frequency vibrations of the test model, and its motion cannot be addressed through digital filtering because a sufficient number of cycles cannot be found during a shock tunnel run. The post-processing of the balance signal thus becomes extremely difficult when an averaging method is employed. Therefore, the force measurement encounters many problems in an impulse facility, particularly for large and heavy models. The objective of the present study is to develop pulse-type sting balance by using a strain-gauge sensor, which can be applied in the force measurement that 100 ms test time, especially for the force test of the large-scale model. Different structures of the S-series (i.e., sting shaped balances) strain-gauge balance are proposed and designed, and the measuring elements are further optimized to overcome the difficulties encountered during the measurement of aerodynamic force in a shock tunnel. In addition, the force tests were conducted using two large-scale test models in JF12, and the S-series strain-gauge balances show good performance in the force measurements during the 100 ms test time.

1 Introduction

For a conventional hypersonic shock tunnel, owing to instantaneous flow field and short test time (generally 500 μs-20 ms) [1–4], the mechanical vibration of the

Y. Wang (✉) · Y. Liu · C. Luo · Z. Jiang
State Key Laboratory of High Temperature Gas Dynamics, Institute of Mechanics, Chinese Academy of Sciences, Beijing, China
e-mail: wangyunpeng@imech.ac.cn

A. Sasoh et al. (eds.), *31st International Symposium on Shock Waves 2*,
https://doi.org/10.1007/978-3-319-91017-8_20

model-balance-support (MBS) system occurs and cannot be damped during a shock tunnel run. For the MBS system, the lowest natural frequency of 1 kHz is sometimes required for the test time of typically 5 ms to obtain improved measurement results [2]. The higher the natural frequencies, the better the justification for the neglected acceleration compensation. For such test conditions, many researchers proposed several special balances to measure the aerodynamic forces in the impulse facilities, that is, accelerometer balance [5–7], stress-wave force balance [8–10], free-flight measurement technique [11–16], and compensated balance [17]. Owing to the very short test time, however, the mature technology was undeveloped for the force measurements in a shock tunnel.

The hypersonic detonation-driven shock tunnel, JF12, was developed based on the backward-running detonation driver technique. Its performance tests demonstrated that the facility is capable of reproducing the pure airflow with Mach numbers from 5 to 9 at altitude of 25–50 km. Based on test duration of more than 100 ms, the stiff construction balance, that is, the traditional internal strain-gauge balance (SGB), was considered for use in the force test in the JF12 long-test-duration impulse facility because of its mature technology and low cost of the strain gauge. However, when the force test is conducted in a shock tunnel, the inertial forces lead to low-frequency vibrations of the model, and its motion cannot be addressed through digital filtering because a sufficient number of cycles cannot be found during a shock tunnel run. This condition implies restriction on the model size and mass as its natural frequencies are inversely proportional the length scale of the model. Based on these technical difficulties, S-series (sting-series) pulse-type SGBs were proposed, and the measuring element structure of SGB was optimized by finite element method (FEM). The maximum loads (i.e., normal force) are from 500 to 12,000 N for the test models with different scales. The finite element computations were performed to analyze the vibrational characteristics of the MBS system to ensure enough cycles of the balance signal and high measuring sensitivity, especially axial element structure, during the 100 ms test. In addition, the force tests were conducted by using two large-scale cones. The S-series SGBs show good performance, and the frequencies of the MBS system increase as a result of the stiff construction of SGB.

2 Strain-Gauge Balances Built at JF12 Shock Tunnel

We used the strain-gauge sensor to measure the aerodynamic loads in the JF12 shock tunnel. The strain-gauge sensor has enough high-frequency response for the force test during a test period of more than 100 ms. The experimental and computational results show that the SGB, with the optimized structures, can be used in this long-test-duration shock tunnel. Therefore, S-series pulse-type SGBs were designed and fabricated for the force tests of JF12.

In this paper, two SGBs, JF12-ISG3-D053-S01 (hereafter referred to as S01) and JF12- ISG6-D106-S03-II (S03-II), are described in detail as the examples of S-series

Table 1 Simultaneous component load ranges (N, Nm)

Serial no.	X	Y	Z	M_x	M_y	M_z
S01	1000	2000	–	–	–	100
S03-II	4000	12,000	12,000	100	400	400

pulse-type SGB. The difference between S01 and S03-II is the element structure of axial load. The balance S01 was further optimized in the aspect of the measuring element of the axial load based on the axial element of S03-II. The performances of S01 and S03-II were examined to determine which type is better for the force measurement in the JF12 shock tunnel.

All the SGBs use only one rectangular beam to measure the components of normal force, side force, yawing moment, and pitching moment. The moment center is located at the center of the rectangular beam. The S01 is a three-component (i.e., axial force X, normal force Y, and pitching moment Mz) sting balance, and the S03-II is the six-component one. Based on the structures of S-series SGB, therefore, four strain gauges are used for the axial load element in the case of S01 and eight strain gauges for the S03-II. These strain-gauge sensors are arranged in a Wheatstone bridge to measure the strain produced by the loads. The output voltage of a balance bridge changes as a function of the strain at the bridge location produced by the applied loads. Table 1 provides details of the load range for two balances used in the present study. The S-series balances with different limited loads are used for the test models with different scales.

3 Design and Optimization of S-Series SGBs

To design and construct a high-stiffness SGB that can meet certain demands, all aspects of the balance technology must be investigated. In this study, only the structure of SGB is considered. From the point of view of structure, these high demands on the balance can be expressed as (1) low interference between each element, (2) high stiffness, (3) low stress level at the strain-gauge positions and related parts, and (4) capability to tolerate errors from the temperature gradients. Among these demands, the important properties for this transport type balance, such as the stiffness, the sensitivity, and the interference, were investigated in the present study.

Owing to the same rectangular beam for measuring Y, Z, M_y, and M_z, the present study focuses on the design and optimization in the axial element structure. To examine the sensitivity performance of the measuring element, the strain computations were conducted in the cases of S01 and S03-II. The findings are shown in Figs. 1 and 2. The first case is the axial force of 1000 N (limited load) acting on the moment center of S01. In this case, the strain output of the axial force element is 336 $\mu\varepsilon$, while the output of the normal force element is only 15 $\mu\varepsilon$. Minimal strain is generated on the rectangular beam when an axial force of 1000 N is applied at the moment center of S01, and vice versa. The effect of the axial force on the

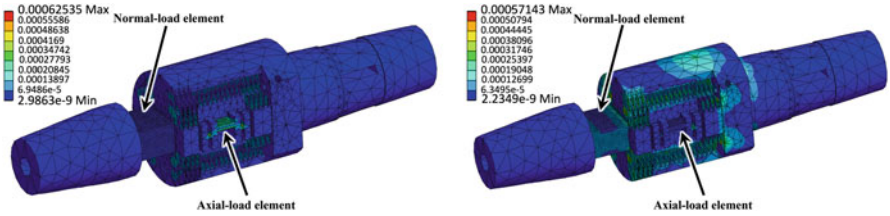

Fig. 1 Strain contours of S01 (left, axial force of 1000 N; right, normal force of 2000 N)

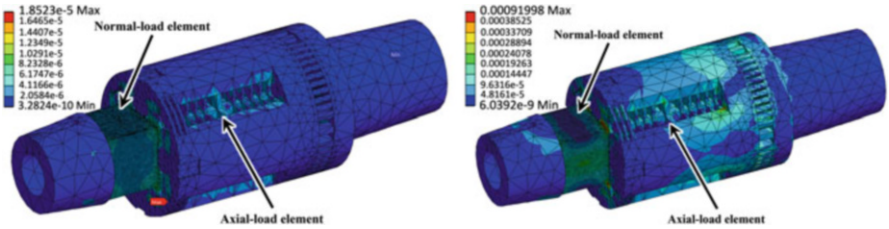

Fig. 2 Strain contours of S03-II (left, axial force of 4000 N; right, normal force of 12,000 N)

Table 2 Combining loading error and repeatability (%)

	Serial no.	X	Y	Z	M_x	M_y	M_z
Error	S01	0.03	0.26	–	–	–	0.12
	S03-II	0.222	0.248	0.38	0.43	0.034	0.054
Repeatability	S01	0.03	0.03	–	–	–	0.05
	S03-II	0.137	0.229	0.256	0.186	0.082	0.071

rectangular beam is very small because of the optimized axial force element. In the S03-II case, however, when the axial force of 4000 N (limited load) is applied at the moment center, the strain of the rectangular element becomes 17 $\mu\varepsilon$ and that of the axial load element is only 40 $\mu\varepsilon$. This result means that the interference of the axial force is larger in the case of S03-II than that of S01. Additionally, the measuring sensitivity of the axial force element of S03-II is also significantly lower than that of S01.

In the same manner, we calculated the cases of the limited normal load acting on S01 and S03-II (see Fig. 2). The case of S01 shows a smaller interference from the normal force where it is less than 5%, while the case of S03-II is more than 70%.

Table 2 shows the calibration performances (i.e., the error and the repeatability) of the S01 and S03-II by the static calibration. The structures of the present balance show good accuracy and precision in the static calibration. The table shows that the axial force of S01 has highest accuracy and precision because of the optimized measuring element. Almost the close errors of the normal force were obtained for the two balances because of the same structure of measuring element, i.e., the rectangular beam.

4 Force Tests

The force tests were conducted in the JF12 shock tunnel to check the performance of the pulse-type sting balances. In the tests, the average stagnation pressure was 2.5 MPa, and the average stagnation temperature was 2200 K. These conditions resulted in an average freestream Mach 7 and an average unit Reynolds number of approximately 0.8×10^6 per meter. In addition, the model was supported by a tail sting mounted on the support mechanism in the test section. The force tests were conducted at nominal angles of attack 5° with zero sideslip angle.

In the experiments, two cones with 10° semivertex angle were used; these were made of aluminum alloy and are 0.75 m and 1.5 m long, respectively (see Fig. 3). The balances S01 and S03-II were used for the smaller and larger cones, respectively, in the force tests. The cone is the standard model and has data available in the literature.

Figure 4 shows the balance voltage signals of the normal force. The case of S03-II shows minimal response (strain output) because of the rectangular beam with large size and high stiffness. Moreover, the frequency of S03-II is also higher than that of S01. The signals were processed at the time range of 96 ms. The two frequencies, i.e., 30.52 Hz and 61.04 Hz, were found using fast Fourier transformation (FFT) analysis in the case of S01. Obviously, at least three cycles can be found during the 100 ms test time. Therefore, the averaging method can be used in the data post-processing.

Additionally, prior to the shock tunnel run, the three-dimensional designs of the MBS system are modeled. A series of computations, including the static structure, dynamics, and modal analysis, is conducted by using FEA. The numerical results can be used to estimate the experimental results, such as the vibrational frequency and cycle number of the MBS system, during the limited test time. Based on FEA of the MBS system, the modal frequencies in the normal direction, 34 and 46 Hz,

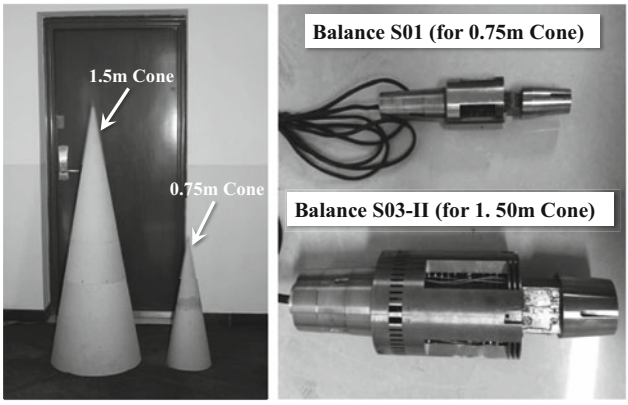

Fig. 3 Two large-scale cones and S-series balances used in the present force tests

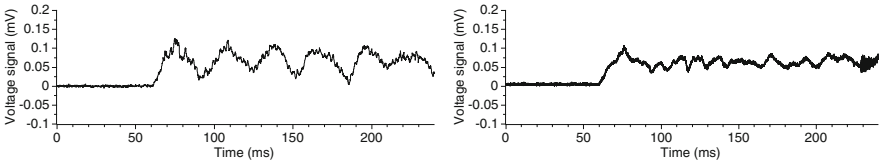

Fig. 4 Voltage signals of normal force by the S01 (left) and S03-II (right)

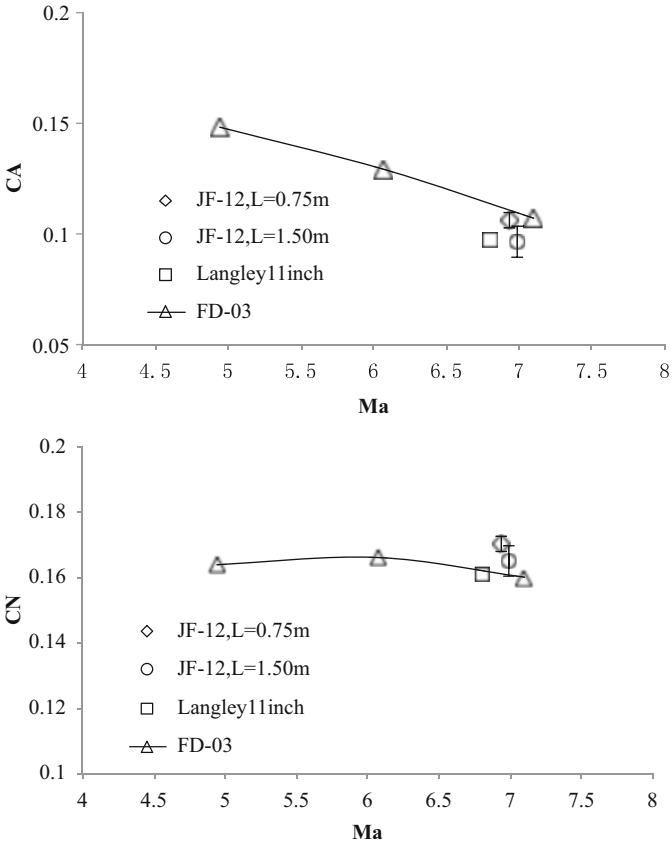

Fig. 5 Aerodynamic coefficient comparison for S01 (0.75 m cone) and S03-II (1.5 m cone)

can be obtained for the cases of S01 and S03-II, respectively. FEM results have a good agreement with the force tests and FEA successfully predicted the vibration performance of the MBSS. In this study, the modal frequency of MBS system, $f \geq 2/t$ Hz (here, t is the test time, e.g., t is approximately 100 ms, then f should be equal and greater than 20 Hz), is used as a design criterion, where at least the two cycles can be found in the balance signal.

Figure 5 presents a comparison of the test results for S01 and S03-II. Some data were obtained by other conventional hypersonic wind tunnels. The results have good

agreement with the data on Langley 11 inch ($T_0 = 630$ K) wind tunnel. In the case of NASA, Mach number is 6.8 and Reynolds number (L) is 0.81×10^6. A comparison with the NASA data shows that the normal and axial force coefficients decreased by 2.61% and 4.69%, respectively, in the case of S01.

5 Conclusion

S-series pulse-type SGBs were designed and optimized for the force tests in the JF12 shock tunnel with long test duration. The range of the maximum load (the normal force of the sting type SGBs) is from 500 to 12,000 N for the test models with different scales. Two sting pulse-type SGBs were compared and analyzed in the aspects of FEM calculation, static calibration, and output signal. The S01, with the optimized axial load element, shows good performance, where its accuracy and precision increase as a result of the higher measuring sensitivity. In addition, the large oscillations of the normal loads have minimal effects on the axial load signal because of the structural optimization. S-series balances were used in the force tests of two large-scale cones in the JF12 shock tunnel. The test results show good agreement with the other wind tunnel data. The structural performance of S-series SGBs fully complies with the requirements of force measurements during 100 ms, especially the measuring capability of the axial load.

Acknowledgments This work was supported by the National Natural Science Foundation of China (Grant No.11672357).

References

1. P.J. Arrington, R.J. Joiner, A.J. Henderson. *Longitudinal Characteristics of Several Configurations at Hypersonic Mach Numbers in Conical and Contoured Nnozzles*, NASA TN D-2489 (1954)
2. L. Bernstein. *Force Measurement in Short-Duration Hypersonic Facilities*. AGARDograph No. 214 (1975)
3. K. Naumann, H. Ende, G. Mathieu, A. George, Millisecond aerodynamic force measurement with side-jet model in the isl shock tunnel. AIAA J. **31**, 1068–1074 (1993)
4. K. Naumann, H. Ende, A novel technique for aerodynamic force measurements in shock tubes. AIP Conf. Proc. **208**, 653–658 (1990)
5. R. Joarder, G. Jagadeesh, A new free floating accelerometer balance system for force measurements in shock tunnels. Shock Waves **13**, 409–412 (2003)
6. S. Saravanan, G. Jagadeesh, K.P.J. Reddy, Aerodynamic force measurement using 3-component accelerometer force balance system in a hypersonic shock tunnel. Shock Waves **18**, 425–435 (2009)
7. N. Sahoo, D.R. Mahapatra, G. Jagadeesh, S. Gopalakrishnan, K.P.J. Reddy, An accelerometer balance system for measurement of aerodynamic force coefficients over blunt bodies in a hypersonic shock tunnel. Meas. Sci. Technol. **14**, 260–272 (2003)

8. M.J. Robinson, J.M. Schramm, K. Hannemann, Design and implementation of an internal stress wave force balance in a shock tunnel. CEAS Space J. **1**, 45–57 (2011)
9. S.R. Sanderson, J.M. Simmons, S.L. Tuttle, A drag measurement technique for free-piston shock tunnels, AIAA Paper 91-0540 (1991)
10. D.J. Mee, W.J.T. Daniel, J.M. Simmons, Three-component force balance for flows of millisecond duration. AIAA J. **34**(3), 590–595 (1996)
11. F. Seiler, G. Mathieu, A. George, J. Srulijes, M. Havermann, Development of a free flight force measuring technique (ffm) at the isl shock tube laboratory, in *25th International Symposium on Shock Wave*, Bangalore, India, 2005
12. P. Wey, M. Bastide, B. Martinez, J. Srulijes, P. Gnemmi, Determination of aerodynamic coeffcients from shock tunnel free- flight trajectories, in *Proceedings of the 28th Aerodynamic Measurement Technology, Ground Testing and Flight Testing Conference*, New Orleans, USA, 2012
13. B. Martinez, M. Bastide, P. Wey, Free-flight measurement technique in shock tunnel, in *Proceedings of the 30th Aerodynamic Measurement Technology and Ground Testing Conference*, Atlanta, USA, 2014
14. H. Tanno, T. Komuro, K. Sato, K. Fujita, S.J. Laurence, Free-flight measurement technique in the free-piston shock tunnel hiest. Rev. Sci. Instrum. **85**, 045112 (2014)
15. H. Tanno, T. Komuro, K. Sato, K. Itoh, T. Yamada, Free-flight tests of reentry capsule models in free-piston shock tunnel, AIAA Paper 2013-2979 (2013)
16. S.J. Laurence, S. Karl, An improved visualization-based force-measurement technique for short-duration hypersonic facilities. Exp. Fluids **48**, 949–965 (2010)
17. E. Marineau, M. MacLean, E. Mundy, M. Holden, Force measurements in hypervelocity flows with an acceleration compensated strain gage balance. J. Spacecr. Rockets **49**(3), 474–482 (2012)